

Possible lateral stress interactions in a sequence of large interplate thrust earthquakes on the subducting Cocos and Rivera plates

Miguel A. Santoyo¹, Takeshi Mikumo¹ and Carlos Mendoza²

¹ *Instituto de Geofísica, Universidad Nacional Autónoma de México, Mexico City, Mexico*

² *Centro de Geociencias, Universidad Nacional Autónoma de México, Campus Juriquilla, Querétaro, Mexico*

Received: July 6, 2006; accepted: July 12, 2007

Resumen

Los grandes sismos en la zona de subducción de México presentan, en ocasiones, agrupamientos espacio-temporales. Ha sido sugerido que dichos agrupamientos pueden ser debidos a la interacción de esfuerzos entre estos eventos. En este trabajo se investiga esta posibilidad mediante el cálculo del cambio en los esfuerzos de Coulomb cosísmicos producidos por siete grandes eventos de subducción ($M_w > 7.4$), ocurridos en una secuencia entre 1973 y 1985 en la placa de Cocos y entre 1995 y 2003 en la placa de Rivera, ambas subducentes bajo la placa de Norte-América. Dichos cálculos están basados en las distribuciones de deslizamientos obtenidas, para estos sismos, mediante previas inversiones cinemáticas. Los cambios de esfuerzos calculados son superpuestos acumulativamente en función del tiempo y el espacio. Los resultados muestran que dichos eventos pueden estar relacionados unos con otros y que, al menos una parte de dicha relación, podría ser atribuida al incremento en los esfuerzos cosísmicos debido a la ocurrencia de grandes eventos previos en zonas adyacentes.

Palabras clave: Sismología, esfuerzos sísmicos, distribución de esfuerzos, convergencia de placas, zona de subducción.

Abstract

Large interplate earthquakes in the Mexican subduction zone may cluster in space and time. This clustering could be due to stress interactions between large events. We investigate this possibility by calculating the coseismic Coulomb failure stress change due to seven large thrust earthquakes ($M_w > 7.4$) that occurred from 1973 to 1985 on the Cocos plate, and from 1995 to 2003 on the Rivera plate subducting beneath the North America plate. The calculations are based on the slip distribution obtained from previous kinematic waveform inversion for these earthquakes. The calculated stress changes are superposed in a cumulative way as a function of time and space. Our results show that these earthquakes could be related to each other. At least part of the relation may possibly be attributed to the coseismic stress increase from the occurrence of previous large events in adjacent zones.

Key words: Seismology, seismic stress, stress distribution, plate convergence, subduction zone.

Introduction

Seismic activity in the Pacific coast of southern Mexico is dominated by the movement of the Cocos and Rivera oceanic plates subducting beneath the continental North America plate. It has been pointed out that large interplate earthquakes in this subduction zone sometimes cluster in space and time (e.g. Singh *et al.*, 1981; Nishenko and Singh, 1987; Ward, 1992). A recent statistical analysis also shows that the observed space-time clustering could be due to possible stress interactions among these large events (Santoyo *et al.*, 2005a). Numerous studies so far have shown that there is a positive correlation between the regions of coseismic stress increase inside and around the source due to a large earthquake and the increment of subsequent seismicity inside these regions (e.g. Reasenberg and Simpson, 1992; King *et al.*, 1994; Deng and Sykes, 1997; Stein *et al.*, 1997; Harris, 1998; Stein, 1999). Some

of these studies also suggested possible triggering of a large earthquake due to previous events with similar magnitudes. It has additionally been suggested that stress increases as small as 0.1 bars could influence subsequent seismicity in the surrounding region of a ruptured fault (e.g. Reasenberg and Simpson, 1992; Deng and Sykes 1997; Stein 1999; Ziv and Rubin, 2000). It is not clear at this moment, however, that this small increase of the Coulomb stress could actually trigger any large earthquakes in the adjacent regions of the subduction zone. Since we are dealing here with large events with magnitudes $M_w > 7.4$ significantly larger than those in the previous studies, we tentatively assume that an increment in the Coulomb stress of the order of at least 0.25 bars would be needed to have an effective influence on subsequent events.

For the Mexican subduction zone, possible stress interactions between large interplate thrust and in-slab

normal-faulting earthquakes have been discussed (Mikumo *et al.*, 1999, 2002). Mikumo *et al.* (1998), also estimated coseismic stress changes during several large thrust earthquakes in this zone and discussed their possible relationship, but their calculations were limited to the shear stress change inside the fault zone. In a previous paper by Santoyo *et al.* (2005a), the space-time clustering of 46 large thrust earthquakes ($M_w > 6.9$) along the Mexican subduction zone during the last 100 years has been investigated with the possible spatial extent of the Coulomb failure stress change based on a simplified slip model. A statistical analysis using the χ^2 -test for the inter-event time intervals between these events indicates the existence of two groups where the observed frequencies are much higher than that expected from a Poisson model, and that the first one with time intervals of 0 – 5 years may be attributed to stress interactions among these large earthquakes.

In the present study, we conduct a more comprehensive analysis using the Coulomb failure stress criterion for a

sequence of large interplate thrust earthquakes ($M_w > 7.4$) that occurred on the Cocos plate during 1973 to 1986 and on the Rivera plate during 1995 to 2003 (Figure 1), to investigate if there is any stress interaction in the lateral direction between these large events.

Data and Method

We estimated the stress change produced by a sequence of seven large ($M_w \geq 7.4$) thrust earthquakes on the plate interface between the subducting Cocos and Rivera plates and the North America plate. The convergence rate of the Cocos plate relative to the North America plate is about 5.2 cm/year in the northwestern section, while it is about 2.5 cm/year for the Rivera plate (DeMets and Wilson, 1997). The boundary between the two plates is uncertain, but it seems to be somewhere near the El Gordo Graben (EGG) (DeMets and Wilson, 1997). Since these two oceanic plates have different convergence rates and directions of motion, we separated our analysis in two parts: one for the five

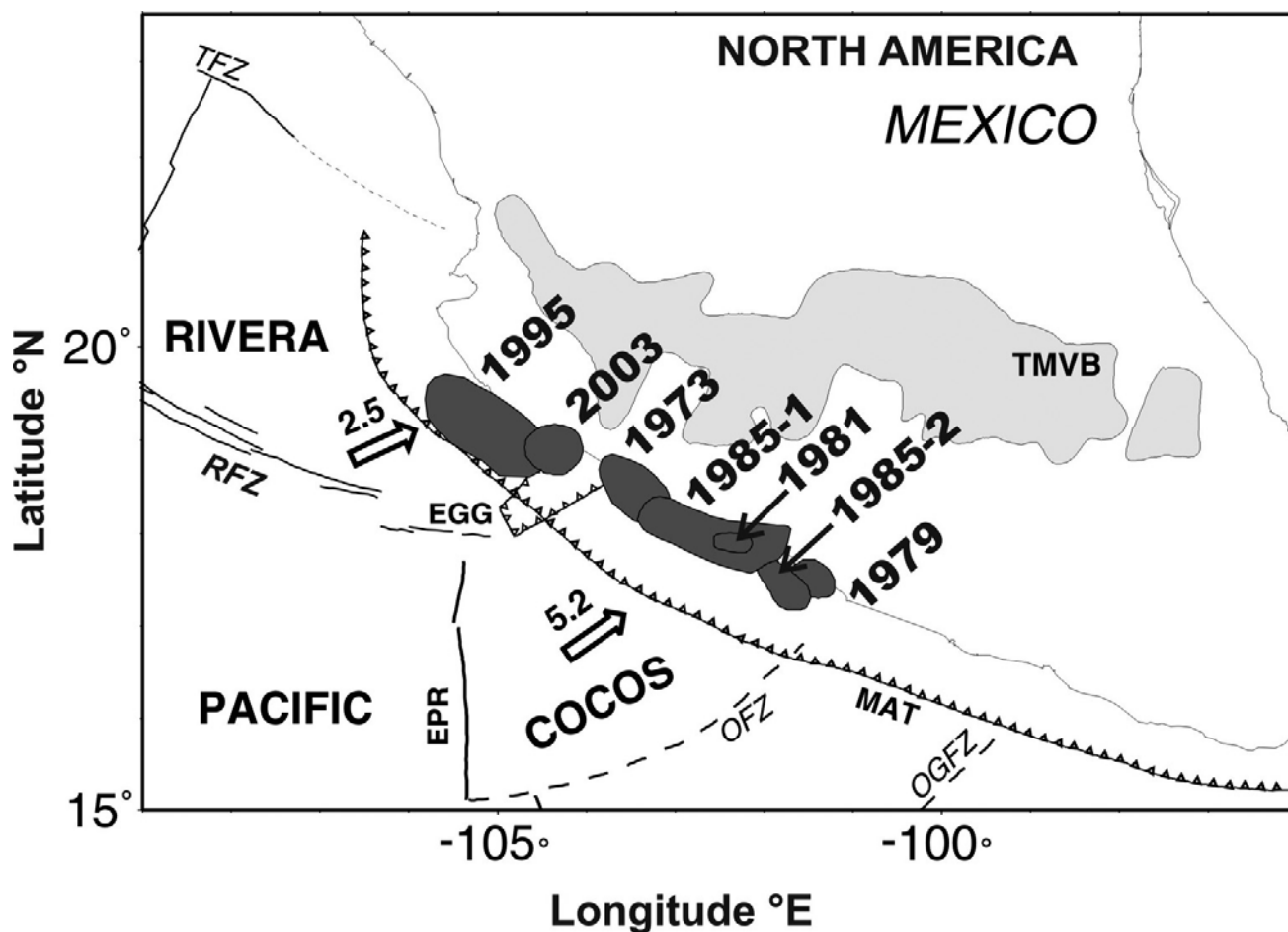


Fig. 1. Tectonic map of the Cocos (COCOS) and Rivera (RIVERA) plates in the Mexican subduction zone and the rupture fault zones of the 7 large earthquakes studied, inferred from their aftershock areas. NORTH AMERICA=North American Plate; PACIFIC=Pacific Plate; RFZ=Rivera Fracture Zone; EPR=East Pacific Rise; EGG=El Gordo Graben; MAT= Middle American Trench. Numerals indicate the year of occurrence of these earthquakes.

events that occurred on the Cocos plate, and another for the two events that occurred on the Rivera plate. Figure 1 shows the ruptured fault zones of the seven large earthquakes inferred mainly from their aftershock area and also the tectonic map of the Cocos and Rivera plates in the Mexican subduction zone. Table 1 gives the source parameters for these events, including the dip, strike and rake that have been obtained from independent fault-plane solution for a point source model from far-field observations. References to these works are also presented in Table 1. It is to be mentioned that the epicentral location of each earthquake may have an uncertainty of about 5 km, so that the relative location between these events may not exceed 10 km.

Slip distribution derived from previous kinematic waveform inversion analysis

The spatial distribution of slip on the fault plane located over the upper plate interface of the subducting plate has been derived in previous kinematic waveform inversion mainly from long-period seismic waves recorded at teleseismic distances during the seven large earthquakes. The results are reproduced in this section.

A. Cocos plate

a. The 30/01/1973 Colima earthquake (Mw=7.6)

The 1973 Colima earthquake occurred on the plate interface between the Cocos and the North America plates, close to the El Gordo Graben. The coseismic slip distribution of this earthquake has been estimated from linear inversion of long-period P-waveforms recorded at

8 WWSSN stations at teleseismic distances, over the fault area of 140 km x 80 km covering depths between 5 and 27 km (Santoyo *et al.*, 2005b). The results obtained are shown in the left-hand side of Figure 2(a), which indicates two large slip zones, one located downdip with a peak slip of about 2.0 m, and the other located updip with a large slip of 1.7 m. It was estimated that the rupture starting from the center of the fault propagated at a velocity of 2.7 km/sec with a source time function of 2.5 sec on each subfault.

b. The 14/03/1979 Petatlán earthquake (Mw=7.6)

The 1979 Petatlán earthquake occurred on the upper interface of the Cocos plate between the Michoacan and Guerrero segments adjacent to the Guerrero seismic gap. The spatial distribution of slip has been inferred from linear waveform inversion of teleseismic P-waves recorded at 6 GDSN and 9 WWSSN stations, over the fault dimension of 120 km x 120 km at the depth range between 2 and 30 km (Mendoza, 1995). In this case a constant rupture velocity of 3.3 km/sec and a box-car type source time function of 1 sec have been obtained. The results are reproduced in the left-hand side of Figure 2(b), which shows a maximum slip of 1.2 m located updip and a slip of 0.7 m near the center of the fault plane.

c. The 25/10/1981 Playa Azul earthquake (Mw=7.4)

The 1981 Playa Azul earthquake took place also on the upper interface of the subducting Cocos plate in the central portion of the Michoacan segment, and is located in between the 1973 Colima and the 1979 Petatlán

Table 1

Source parameters for the earthquakes studied

No.	Earthquake	Date(D,M,Y)	Lat(°N) [§]	Lon(°E) [§]	Mw [◆]	Mech. (θ, δ, λ) [♣]	P.I. [*]	Ref [†]
1	Colima	30/01/1973	18.39	-103.21	7.6	305°, 16°, 93°	C	α
2	Petatlán	14/03/1979	17.46	-101.46	7.6	293°, 15°, 105°	C	β
3	Playa Azul	25/10/1981	17.75	-102.25	7.4	287°, 20°, 82°	C	γ
4	Michoacan	19/09/1985	18.14	-102.71	8.1	300°, 14°, 89°	C	δ
5	Zihuatanejo	21/09/1985	17.62	-101.82	7.6	296°, 17°, 85°	C	γ
6	M. Aftershock [‡]	30/04/1986	18.42	-102.99	7.1	290°, 18°, 87°	C	---
7	Colima-Jalisco	09/10/1995	18.84	-104.58	8.0	309°, 14°, 92°	R	ε
8	Tecomán	22/01/2003	18.71	-104.13	7.5	300°, 20°, 93°	R	ζ

Notes: §Locations are taken from references listed below except for event 6 which is from Singh and Mortera, (1991); Lat=Latitude North, Lon=Longitude East. ◆Mw=Moment magnitude. ♣Mech=Focal mechanism (θ=Strike, δ=Dip, λ=rake) from references shown in the last column, except event 6 from CMT Harvard. *P.I.= Plate Interface, where C=Cocos, R=Rivera. †References for slip distributions: α. Santoyo, *et al.* (2005b); β. Mendoza, (1995); γ. Mendoza, (1993); δ. Mendoza and Hartzell, (1989); ε. Mendoza and Hartzell, (1997); ζ. Yagi, *et al.* (2004). ‡Aftershock belonging to the Michoacan 19/09/1985 earthquake.

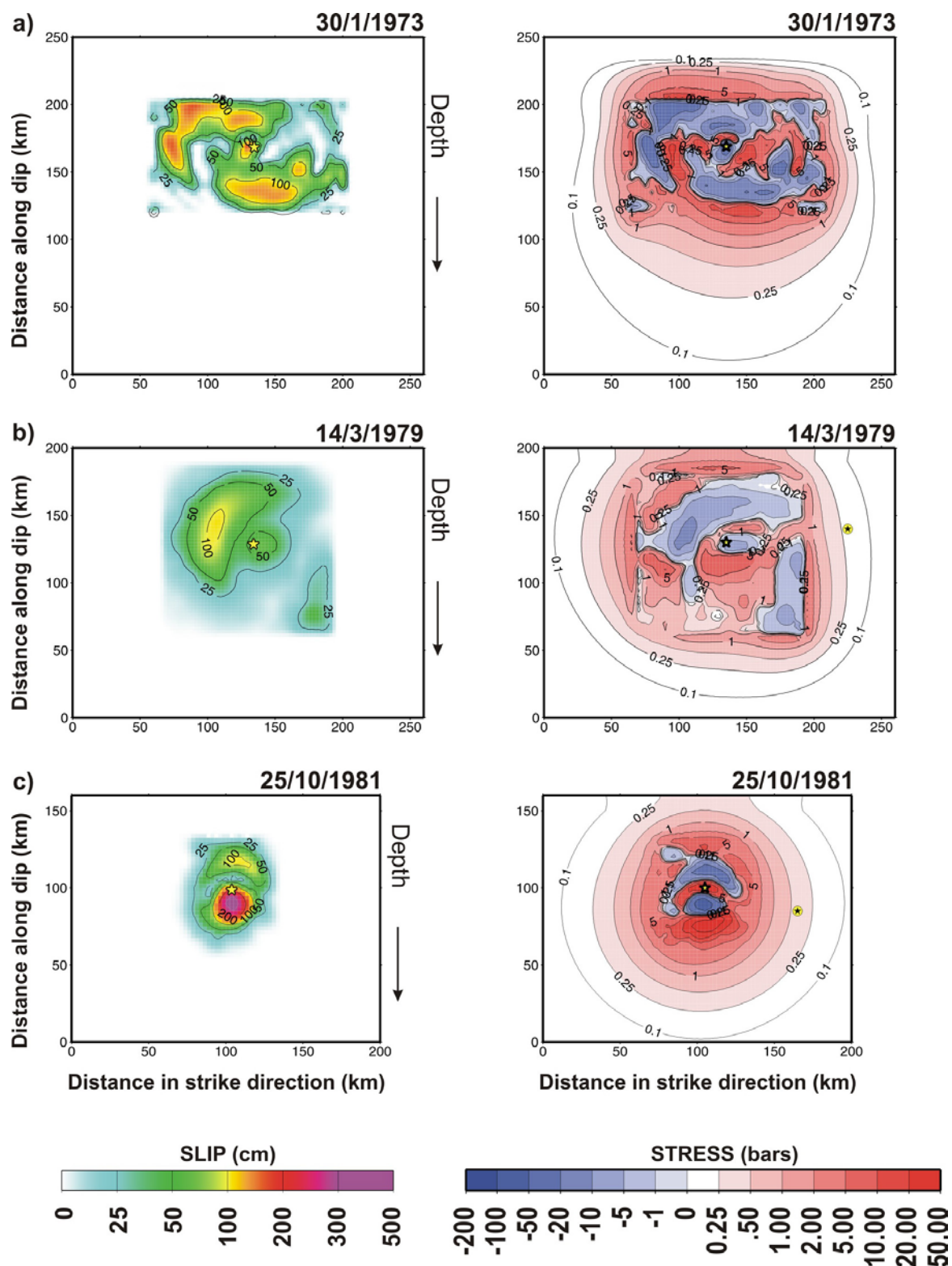


Fig. 2. Slip distribution and coseismic stress change for the five studied earthquakes occurred on the Cocos plate. Left hand side: slip distribution over the fault plane of each studied earthquake, derived from kinematic waveform inversion; Right hand side: coseismic change of the Coulomb failure stress (ΔCFS) distribution, calculated from the slip distributions shown at the right-hand side. The title above frames identify the earthquakes: a) 1973, Colima, b) 1979, Petatlán, c) 1981, Playa Azul, d) 1985, Michoacan, and e) 1985, Zihuatanejo earthquakes. The yellow star indicates the hypocentral location of each event and the black star inside a yellow circle indicates the hypocentral location of the following large earthquake.

earthquakes. A linear waveform inversion has been applied to teleseismic P-waves recorded at 15 GDSN and WWSSN stations to estimate the slip distribution over the fault at depths between 6 and 23 km (Mendoza, 1993). The inversion has been made with a triangular source time function of 1 sec and a constant rupture velocity of 2.6 km/sec. The results are reproduced in the left-hand side of Figure 2(c), which indicates a peak slip of 3.5 m concentrated below the hypocenter and a large slip of 1.0 m located updip.

d. The 19/09/1985 Michoacan earthquake (Mw=8.1)

The 1985 Michoacan earthquake was the greatest earthquake in the Mexican subduction zone since 1932, and ruptured most of the Michoacan segment of the Cocos – North America plate boundary. This event is located in

between the ruptured zones of the 1973 Colima and the 1979 Petatlán earthquakes, and covers the source area of the 1981 Playa Azul earthquake. The spatial distribution of slip during this unusually large earthquake has been estimated from waveform inversion of 4 near-source strong motion records and P-waves recorded at 13 teleseismic stations, over the fault plane with a dimension of 180 km x 140 km covering the depth range between 6 and 40 km (Mendoza and Hartzell, 1989). It was found that the rupture propagated at a constant velocity of 2.6 km with a 2 sec triangular source time function. The results are reproduced in the left-hand side of Figure 2(d), indicating three major slip zones: one with a maximum slip of 6.5 m in a zone of 80 km x 50 km near the hypocenter, another with a peak slip of 5.0 m in a 45 km x 60 km area in the southwest portion, and the last one with a peak slip of 3.0 m in a 30 km x 60 km area in the downdip portion.

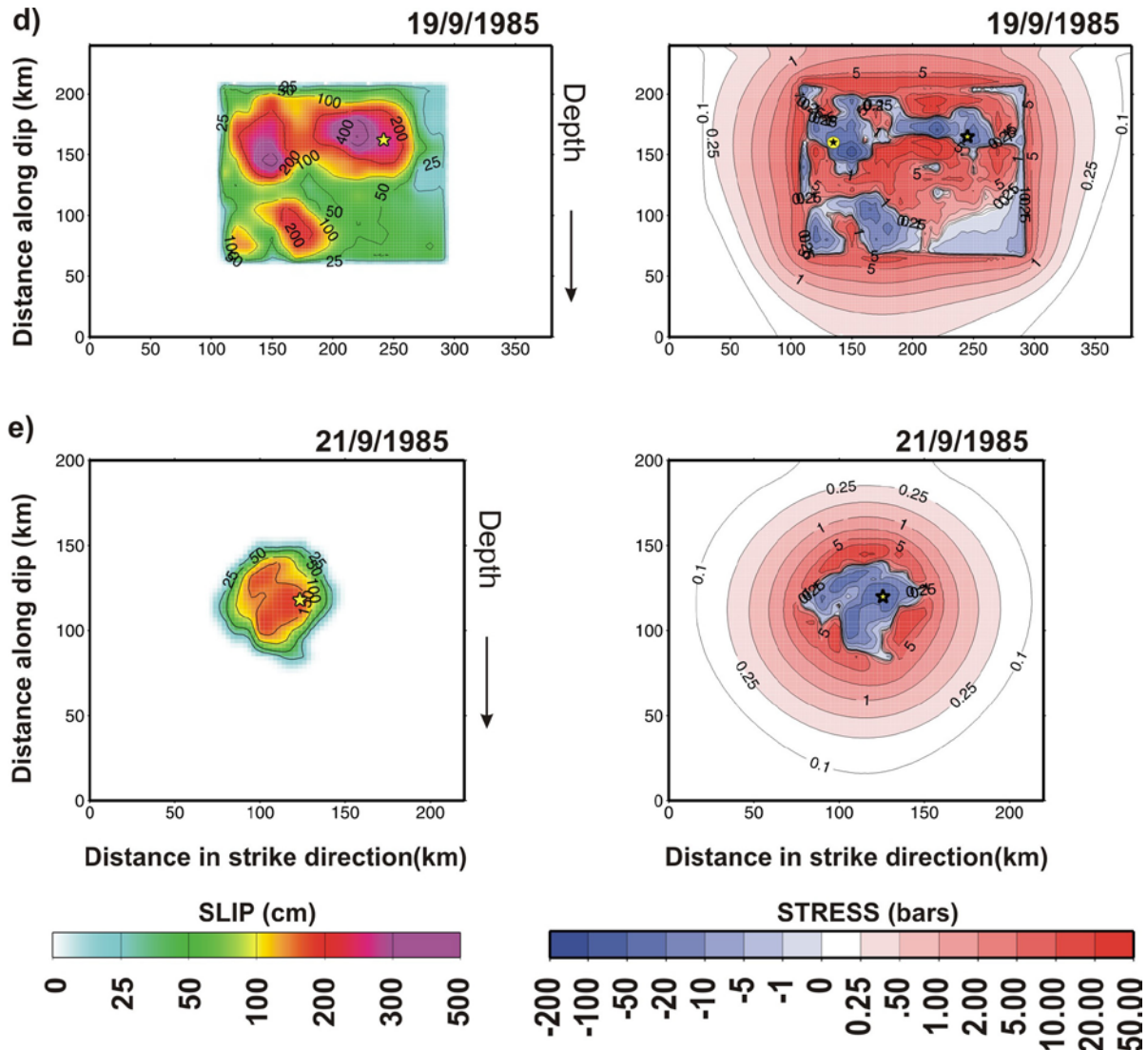


Fig. 2. Continued.

e. The 21/09/1985 Zihuatanejo earthquake (Mw=7.6)

The 1985 Zihuatanejo earthquake occurred two days later as the largest aftershock, immediately southeast of the ruptured zone of the 19/09/1985 largest event. The waveform inversion of P and SH waves recorded at 16 GDSN teleseismic stations has been made with the same source time function as in the case of the 1981 Playa Azul event (Mendoza, 1993). The slip distribution reproduced in Figure 2(e) shows a peak slip of 1.7 m and 2.0 m in a circular zone with a radius of about 30 km over a fault dimension of 90 km x 90 km covering the depth range between 12 and 26 km.

B. Rivera plate

a. The 09/10/1995 Colima-Jalisco earthquake (Mw=8.0)

The 1995 Colima-Jalisco earthquake was the largest earthquake that occurred on the Rivera – North America plate boundary since the 1932 great Jalisco earthquake (Singh *et al.*, 1985). The slip distribution has been estimated by waveform inversion of broadband P-waves recorded at 38 GDSN stations at teleseismic distances, using a rupture velocity of 2.8 km/sec and a 2-sec box-car source time function (Mendoza and Hartzell, 1997). The results reproduced in Figure 3(a) indicate 3 large slip zones, with a peak slip exceeding 4.5 and 4.8 m, located at two shallow updip portions and a significant slip larger than 1.5 m near the hypocenter, over a fault dimension of 200 km x 100 km covering depths between 3 and 27 km. A similar waveform inversion has been made, incorporating 2 near-source strong motion records and P-waves at 15 selected teleseismic stations (Yagi, personal communication, 2004). The results show more minor details but generally similar patterns. Melbourne, *et al.* (1997) also calculated the slip distribution on the fault plane of this earthquake. This distribution derived only from several GPS measurements over quite a long time before and after this event does not appear to be well resolved nor to be able to account for seismic wave observations. Ortiz, *et al.* (2000), based on Tsunami recordings, gives additional constraints on the earthquake uplift and concludes that the Mendoza and Hartzell (1977) model is more consistent with the Tsunami data than other inversions.

b. The 22/01/2003 Tecmán, Colima, earthquake (Mw=7.5)

The 2003 Tecmán, Colima, earthquake occurred near the boundary between the Rivera and Cocos plates both subducting beneath the North America plate. The ruptured fault zone appears to partially overlap the southeastern fault section of the 1995 Colima-Jalisco earthquake, breaking part of the El Gordo Graben, but did not reach the ruptured

zone of the 1973 Colima earthquake. A waveform inversion has been made incorporating 6 near-source strong-motion records and 14 teleseismic P and SH waves (Yagi *et al.*, 2004). The results are reproduced in the left-side of Figure 3(b), indicating two major slip zones, one being located near the center of the fault with a peak slip of 3.4 m and another located downdip with a large slip of 3.1 m, over the fault plane with a dimension of 35 km x 70 km, covering depths between 2 and 30 km.

Although, as described above, slightly different rupture velocities and source time functions have been obtained for each of the above earthquakes, these parameters provided the best fit between the synthetic and observed seismograms after having searched for some possible ranges. It should also be mentioned here that there is some intrinsic resolution uncertainties in all the slip distributions shown above. Since most of the kinematic waveform inversions are limited to wave frequencies lower than 0.5 Hz, the spatial resolution of the slip may be between 5 ~ 6 km for rupture velocities ranging between 2.5 and 3.0 km/sec. This would also affect the boundaries between the zones of stress decrease and increase, which will be shown in the next section.

Coseismic change in the Coulomb failure stress

We computed the coseismic Coulomb failure stress change (ΔCFS) inside and in the vicinity of the fault area on the plate interface from the slip distribution for each event. The change in the Coulomb failure stress is obtained from the relation $\Delta CFS = \Delta \tau + \mu' \Delta \sigma_n$ (e.g. Harris, 1998), where $\Delta \tau$ is the shear stress change in the direction of the fault slip, $\Delta \sigma_n$ is the change in the tensional stress normal to the fault plane, and μ' is an apparent coefficient of friction $\mu' = \mu (1 - p)$, μ is the static coefficient of friction and p is the pore pressure in the source volume.

All these stresses were calculated in a tensorial way for a 3D horizontally-layered model (Table 2) by the finite difference scheme, as well as for a half space model using the formulations given by Okada (1992). In this calculation, we refer to the fault dimension assigned in the kinematic waveform inversion with a size of divided subfaults of 5km x 5km for all the earthquakes. In the latter computations, we assumed a mean shear modulus of $\mu = 3.5 \times 10^{11}$ dyn/cm², and a Poisson ratio of $\nu = 0.25$ for the region. For the apparent coefficient of friction, we tested different values ranging from 0.2 to 0.6, and finally used the value of $\mu' = 0.4$ adopted by Mikumo *et al.* (1999; 2002) for the Mexican subduction zone. In the cases of the 19/09/1985 Michoacan and 9/10/1995 Colima-Jalisco events, the inversion results yielded relatively high slips near the fault edges, which generate some edge effects in the stress distribution. In

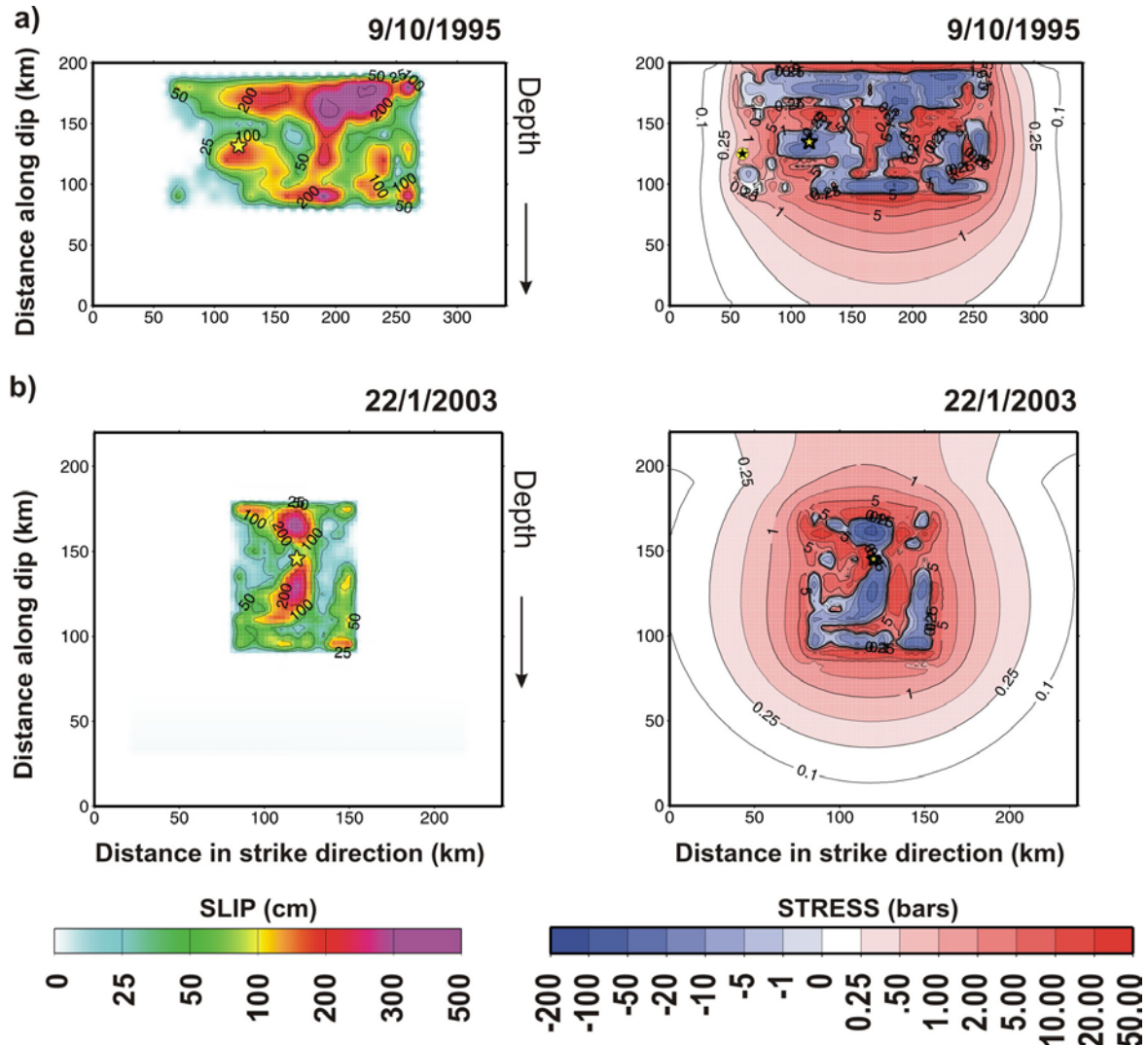


Fig. 3. Slip distribution and coseismic stress change for the two studied earthquakes occurred on the Rivera plate. Left hand side: slip distribution over the fault plane of each studied earthquake, derived from kinematic waveform inversion; Right hand side: coseismic change of the Coulomb failure stress (Δ CFS) distribution, calculated from the slip distribution at the right-hand side. The title above frames identify the earthquakes: a) 1995, Colima-Jalisco, and b) 2003, Tecoman, Colima earthquakes. Yellow star indicates the hypocentral location of each event and the black star inside a yellow circle indicates the hypocentral location of the following large earthquake.

order to suppress these edge effects, we applied a cosine taper function of 2% over the total fault length and width in the two spatial directions.

As the focal parameters given in Table 1 are slightly different for each earthquake, we adopted in the computation of the Δ CFS function a general value of the strike and dip angles based on the geometry of the Benioff zone of each subducting plate (Pardo and Suárez, 1995). For five earthquakes on the Cocos plate we used a strike value of $\theta=290^\circ$ and for two earthquakes on the Rivera plate a strike value of $\theta=300^\circ$. We assigned a dip value of $\delta=15^\circ$ and a rake value of $\lambda=90^\circ$ for all the earthquakes. Based on the extent of the fault areas from the kinematic

model dimensions of the studied earthquakes, we take a rectangular plate interface covering an area of 475km x 240m for the Cocos plate, and for the Rivera plate we take an area of 390km x 240km. In both cases we used a mesh size of 2.0km x 2.0km for the location of the computation points. The calculated changes of Δ CFS due to each of the seven earthquakes are shown separately at the right-hand side of Figures 2 and 3, on the Cocos and Rivera plates respectively. It should be mentioned that if we assume different apparent friction coefficients $\mu' = 0.2$ or $\mu' = 0.6$ instead of its average value of 0.4, the absolute values of Δ CFS calculated above changed by an average of 20 % with a maximum of 70 % depending on the location inside the ruptured fault zone, but were not much affected by the

Table 2

Crust and upper mantle structure used in this study

Layer	H (km)	Vp (km/s)	Vs (km/s)	ρ (g/cm ³)
I	0	5.80	3.35	2.68
II	6	6.40	3.69	2.78
III	25	7.00	4.04	2.85
IV	35	8.00	4.62	3.00

Notes: Horizontally-layered structure for the Michoacan region based on Mendoza and Hartzell (1989); H: Top depth to each layer, Vp: P-wave velocity, Vs: S-wave velocity, ρ : layer density.

choice of μ' outside the ruptured zone. Additionally, we made tests for the effects of the fault geometry of each earthquake on the change of the Coulomb failure stress over the extended plane. We found that the variation of the Δ CFS in lateral direction is 3% at most with respect to those computed for the assumed geometry. A schematic view of the fault geometry with respect to the subduction zone structure is shown in Figure 4.

To account for the contribution from each earthquake to the total state of stress on the plate interface, we summed up, as a next step, the calculated stress due to each earthquake, setting the state of stress before the first event in the sequence on each plate to be zero. The relative locations between the events studied here were based on their epicentral locations. Finally, the state of stress over

the fault interface is presented in a cumulative way as a function of time.

Cocos plate

In the right-hand side of Figure 2a, we present the change of Δ CFS over the plate interface due to the Colima earthquake of 30/01/1973 ($M_w=7.6$). The epicenter of this earthquake is denoted by a yellow star. Red contours show the zones of stress increase and blue ones indicate the zones of stress drop. In Figure 5a we show the same Δ CFS for this event in a map horizontal projection. The epicenter of the next event in the sequence is denoted by a black star in a yellow circle. This event ruptured two main asperities, one on the southeastern section of the fault with a maximum stress drop of -45 bars, and another one on the northwestern section of the fault with a maximum stress drop of -37 bars. The maximum stress increase of 19 bars occurred between these two asperities about 60 km southeast of the epicenter. Here it can be observed that the epicenter of the next large earthquake (Petatlán 1979) falls approximately 130 km to the southeastern edge of the fault zone, and far outside the 0.25-bar contour due to the 1973 earthquake. This indicates that the 1979 event was hardly affected by the static stress change due to the 1973 event.

The next earthquake in the sequence is the Petatlán earthquake of 14/03/1979 ($M_w=7.6$) (right-hand side of Figure 2b and Figure 5b). This event had two main asperities, with a maximum stress drop of -12 bars located 30 km southeast of its epicenter. It can now be observed that the 0.25 bar-contour from this event reaches the contour of

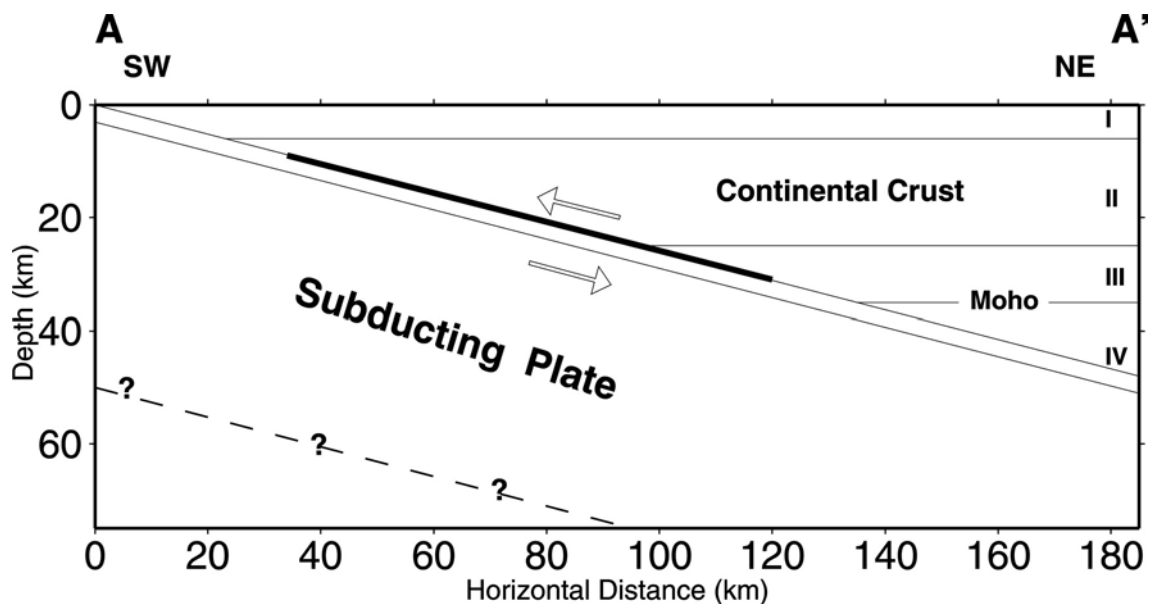


Fig. 4. 2-D cross section of the Mexican subduction zone structure and fault geometry assumed. Layers I and II=upper crust; III= lower crust and IV=upper mantle. The elastic parameters for the structure are given in Table 2. The fault plane interface is shown with a thick black line.

the same value due to the previous 1973 event. Here the epicenter of the third event in the sequence (Playa Azul, 1981) falls in between these two contours. This suggests that stress due to both of the 1973 and 1979 events, provides triggering effects on the occurrence of the 1981 earthquake.

The Playa Azul earthquake of 25/10/1981 (Mw=7.4) is the third and smallest earthquake in the sequence, but produced the highest stress drop on two asperities, located on the northern and southern sides of the epicenter (right-hand side of Figure 2c and Figure 5c) with a maximum of -180 bars. The maximum stress increase occurred in between of the two asperities, with a value of 55 bars. These high values are mostly due to large slips (~350 cm) concentrated on a relatively small area. Because of its location between the previous two events, this earthquake has a strong positive influence on its adjacent zones, increasing the state of stress of the southeastern asperity of the 1973 earthquake as well as the northwestern side of the 1979 fault. Since the epicenter of the 1985 Michoacan earthquake (Mw=8.1) is located inside the zone of increased stress due to the 1973 and 1981 events, the great earthquake appears to have been affected by both of the two events.

The great 1985 Michoacan earthquake (19/09/1985) with a moment magnitude of Mw=8.1 is the largest and most damaging earthquake in the sequence. As we mentioned above, this earthquake may have been affected by the stress increase due to the 1973 and 1981 earthquakes. This event ruptured two main asperities and one large patch, where the largest asperity occurred just to the southeast of the epicenter (right-hand side of Figure 2d and Figure 5d). This asperity produced a maximum stress drop of -120 bars, and a maximum stress increase of 23 bars. This event effectively affects the areas of stress influence from the three previous events. The combined stress changes due to these four events produced different spots of stress increase especially near the epicentral region of the 1981 Playa Azul earthquake, where the stress increase reaches a positive value of 83 bars.

The following event in the sequence on the Cocos plate is the Zihuatanejo earthquake of 21/09/1985 (Mw=7.6). The epicenter of this event appears to be located inside the zone of stress drop but very close to the zone of stress increase (right-hand side of Figure 2e and Figure 5e). However, there could be a small mislocation of the epicenter of this event, or inherent uncertainties in the slip distribution in the previous 1985 event.

Another large aftershock (Mw=7.1) of the 1985 event also occurred on 30/04/1986. Its epicenter is located in the ruptured area of the 1985 event (18.42°N, -102.99°E) inside

a positive 1.0 bar-contour, which also suggests a possible triggering effect on this aftershock.

Rivera Plate

This plate had generated two successive large earthquakes (3/06/1932, Mw=8.2 and 18/06/1932 Mw=7.8) in the first half of the past century (Singh, *et al.*, 1985). It seems unlikely, however, that these events more than 70 years ago provided a direct stress influence to the present.

The first event analyzed here is the 9/10/1995 Colima-Jalisco (Mw=8.0) earthquake. As in the previous analysis, we set the state of stress before this event to be zero. As shown in the right-hand side of Figure 3a and Figure 6a, this event ruptured three main asperities; one is located on the epicentral zone and the other two on the northwest side of the epicenter, very close to the Middle America trench. The maximum stress drop of -170 bars occurred inside the largest asperity on the northwestern edge of the fault, and the second largest stress drop of -155 bars occurred on the southeastern asperity. The largest stress increase due to this earthquake is located in between the second largest and the epicentral asperities, with a maximum value of 17 bars. The next event in this sequence (Tecomán, 2003), whose epicenter is shown by a black star in a yellow circle, falls clearly inside the zone of positive stress change produced by the 1995 earthquake, in the southeastern side of its fault within a 1.0 bar contour. In this case it seems clear that the zone of stress increase due to the 1995 event provided a triggering effect on the 2003 event.

The next event in this sequence is the 22/01/2003 Tecomán (Mw=7.5) earthquake (right-hand side of Figure 3b and Figure 6b). This event ruptured two main asperities and produced a maximum stress drop of -65 bars and a maximum stress increase of about 20 bars. Here, the combined stress change due to these two events produced a relatively high stress increase zone between the two epicenters with a maximum value of 37 bars. This last event appears to have occurred in part of the Graben "El Gordo", where the occurrence of large earthquakes was unknown until this earthquake.

As can be observed in Figures 5d and 6b, the stress change due to the two events on the Rivera plate could have some effect on a possible future event on the Cocos plate; also, the stress increase due to the 1973 and 1985 events on the Cocos plate could affect the sequence of earthquakes on the Rivera plate. These observations, however, should be taken with some care due to the uncertainties of the limits between these two oceanic plates and their related tectonic environments.

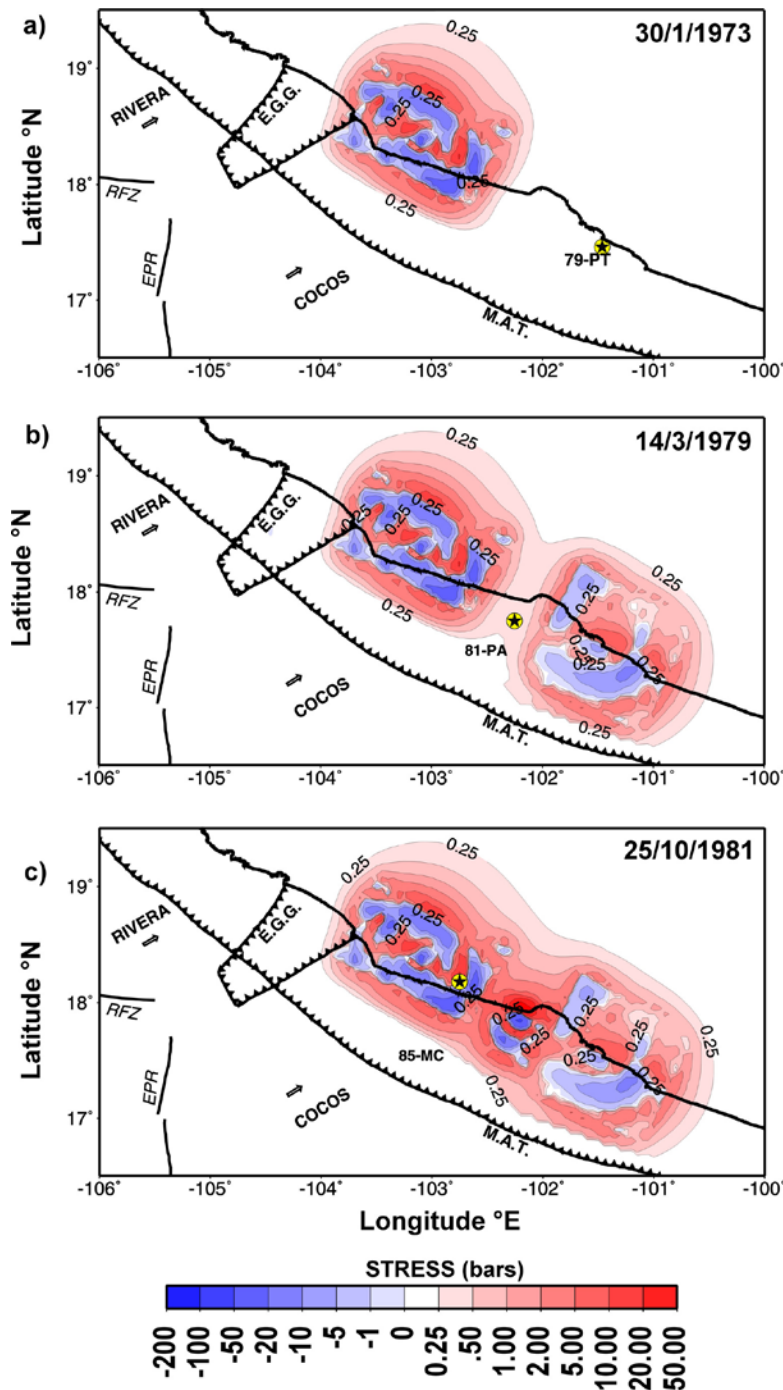


Fig. 5. Coseismic Coulomb stress changes in the Cocos plate, due to the sequence of earthquakes between 1973 and 1985 studied in this work. The grid size discretization used for the observation plane, where coseismic stress changes were computed, is 2.0 km x 2.0 km over the fault plane. Results are presented on a map view of the fault plane projected on a horizontal plane, as a function of time, taken from Figures 2(a)-2(e). Blue zones denote stress drops and red zones denote stress increases following the scale shown in the bottom of the figure. The time of its occurrence is shown at the upper-right side of each figure (see Table 1 for details of each earthquake). Black star in a yellow circle show the epicentral location of the next earthquake of the sequence. Tectonic features are the same as described in Figure 1. For details of the source characteristics of each earthquake, see Table 1. Stress changes in the scale are shown in bars. a) Coseismic Coulomb stress change associated with the 1973 Colima earthquake. b) Coulomb stress evolution after the occurrence of the 1979 Petatlán earthquake. c) State of the stress up to the occurrence of the 1981 Playa Azul earthquake. d) Stress changes after the great 1985 Michoacan earthquake. e) Final state of stress in this sequence after the 1985 Zihuatanejo earthquake. Note that the epicenter of the 1986 aftershock is located in the stress increase zone due to the summed effects of the four previous events.

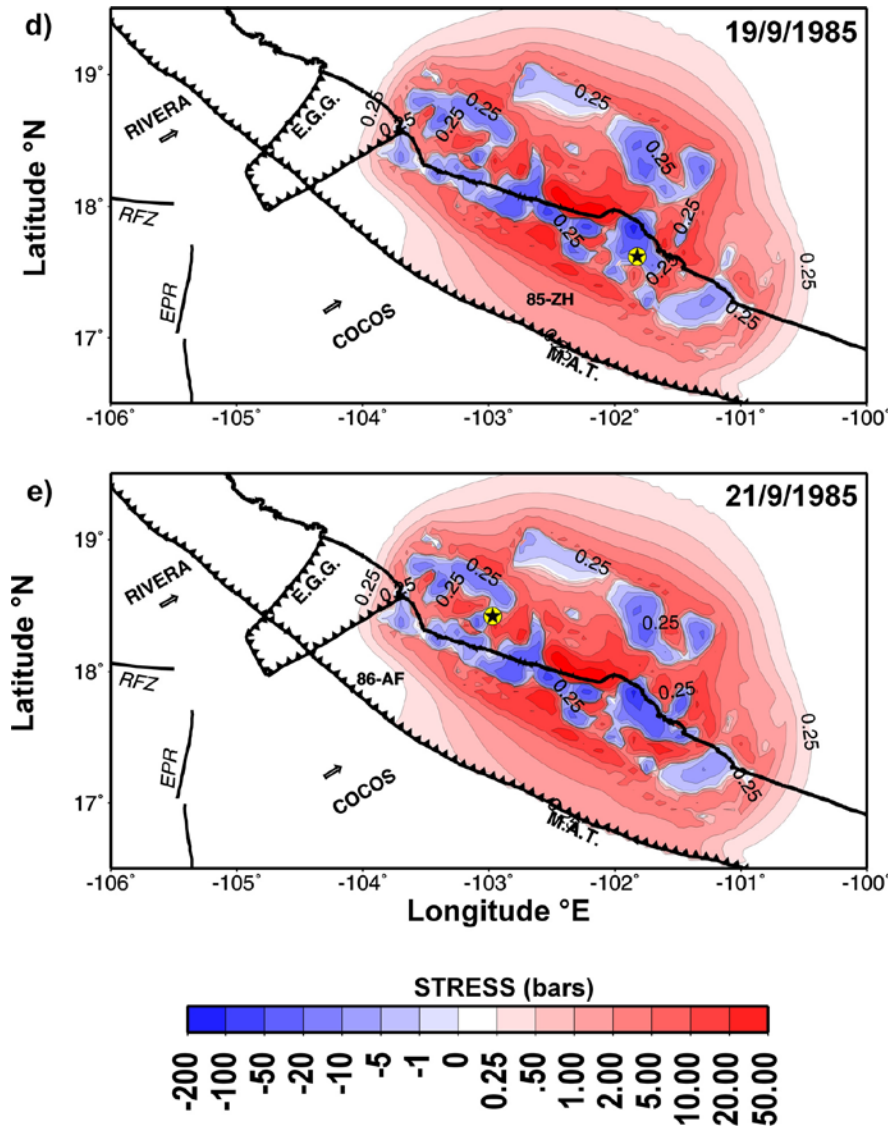


Fig. 5. Continued

Discussion

The above discussion is based entirely on the coseismic change of Coulomb failure stress. Under more realistic environments, however, there should be postseismic stress change caused by some time dependent tectonic processes. The main factors that could affect the coseismic change on the plate interface may be viscoelastic relaxation process in the lower mantle and in the asthenosphere underlying the subducting slab, tectonic loading of stress due to plate convergence, and also possible postseismic slow slip that could occur adjacent to or around the ruptured fault zone.

The postseismic viscoelastic stress change has been discussed in previous work, for crustal strike-slip or dip-slip

earthquakes (e.g. Freed and Lin, 1998; Pollitz *et al.*, 2000; Pollitz and Sacks, 2002), and for thrust earthquakes around subduction zones (e.g. Thatcher and Rundle, 1984; Rydelek and Sacks, 1990; Dmowska *et al.*, 1996; Taylor *et al.*, 1998; Mikumo *et al.*, 2002). These studies dealt mainly with stress change on horizontal cross sections in the crust or on a vertical cross section including a vertical or a dipping fault within the crust and upper mantle, indicating significant viscoelastic effects for long time range. On the other hand, however, we are interested in postseismic stress change in the ruptured fault zone and particularly in its adjacent and surrounding zones on the plate interface, to see how much lateral stress diffusion would take place.

It has been shown in a recent result from 3D finite-element viscoelastic models dealing with possible

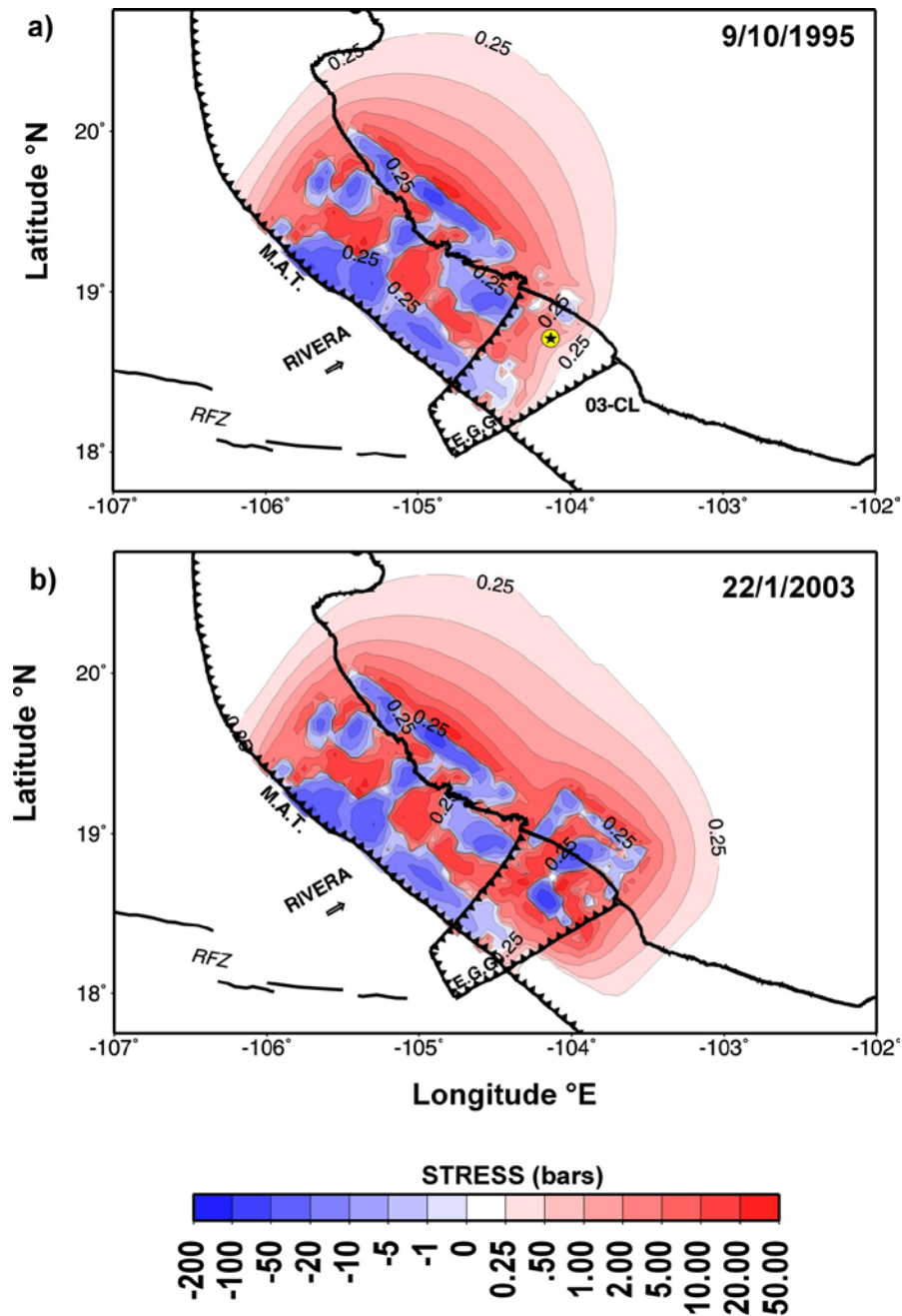


Fig. 6. Coseismic Coulomb stress changes in the Rivera plate, due to the sequence of earthquakes between 1995 and 2003 studied in this work. These results are given on a map view of the fault plane projected on a horizontal plane, as a function of time, taken from Figures 3(a) and 3(b). Figure notes are the same as for Figure 5. a) Coseismic Coulomb stress change due to the 1995 Colima-Jalisco earthquake. b) State of stress after the occurrence of the 2003 Tecmán earthquake.

lateral propagation of a slow slip event in the Mexican subduction zone (A. Shiraishi and S. Yoshioka, personal communication, 2005) that the viscoelastic effects in this specific case appear quite small in these adjacent zones and yield only very weak lateral stress diffusion. The possible existence of lateral stress diffusion has been suggested (Anderson, 1975), and actually demonstrated (e.g. Rice, 1980; Lehner *et al.*, 1981) for plane stress deformation in an

elastic lithosphere overlying a viscoelastic asthenosphere. The difference between the recent result and these previous calculations might come from some difference in the direction of the applied stress with respect to the assumed fault geometry or in the depth variation of elastic and viscoelastic properties. We are now making quantitative estimates for the postseismic stress changes due to the viscoelastic relaxation process and the recovery of tectonic

loading, and the results will be reported in a separate paper.

In the present study, it was found that the rupture nucleation zone of a subsequent event, except possibly the 1985 Zihuatanejo event, appears to be located in the zone of stress increase due to its previous event. There is a possibility, however, that there could be inherent small uncertainties less than 10 km or so in the relative epicentral location of two events. Another problem is some intrinsic resolution uncertainties in the slip distributions up to about 5 ~ 6 km, and also some possible effects from not well-known apparent coefficient of friction. The Zihuatanejo event, which was the largest aftershock of the 1985 great Michoacan earthquake, should have been most affected by the mainshock event, but its epicenter appears to be located inside the zone of stress decrease, or at best near the boundary between the zones of stress decrease and increase due to the Michoacan event. This might be attributed to the above-mentioned problems, but is still unsolved. The same problem could be present also in the other cases dealt with in this paper. For these reasons, the above inference on the location of the rupture nucleation zone may not be conclusive but should be regarded as a possibility.

Although these uncertainties remain, the spatio-temporal clustering of large earthquakes in this subduction zone may be mainly accounted for by coseismic stress increase due to the preceding events that occurred in adjacent segments. In this case, the relatively short time interval between these large events may depend on some difference between the current state of stress at a given time and the frictional strength on specific segments of the plate interface. The current stress includes the ambient tectonic stress level and its coseismic and postseismic stress changes, which are heterogeneous. On the other hand, the frictional strength could also be spatially heterogeneous, depending on the roughness of the interface, the lithospheric environment (including temperature, pore pressure, humidity, etc.), and also on other time-dependent factors. One of the possible mechanisms would be a classical stress corrosion mechanism due to static fatigue of fault zone materials often experienced in laboratory experiments (e.g. Anderson and Grew, 1977). Another possibility would be the delayed occurrence of triggered events due to time-dependent frictional response of fault materials under the applied stress perturbations. (e.g. Voisin *et al.*, 2004; Kato, 2004). It is probable that if any segment on the plate interface received coseismic stress increase from its adjacent segments, then they could be ruptured during a relatively short time interval.

On the other hand, if afterslip actually occurred adjacent to or around the coseismic ruptured zones of the large

earthquakes mentioned in this article, such as after the 1994 Off-Sanriku (Heki *et al.*, 1997; Yagi *et al.*, 2003), 1996 Hyuganada (Hirose *et al.*, 1999), and 2003 Off-Tokachi (Miyazaki *et al.*, 2004; Baba *et al.*, 2005) earthquakes around the Japanese Islands, the postseismic stress change would extend further outside the ruptured zone. Clear evidence of afterslip has not been detected in the Mexican subduction zone, however, due to the lack of geodetic observations at that time. There is also another possibility that relatively large- and medium-size aftershocks of these large earthquakes could modify the stress patterns to some extent (e.g. Harris and Simpson, 2002) and hence could affect the time intervals shown here. In all cases, however, the coseismic stress change may play an important role in the triggering of large earthquakes in adjacent zones.

Conclusions

We have investigated the possibility of lateral stress interactions along the Mexican subduction zone, in a sequence of large interplate earthquakes ($M_w > 7.4$) that occurred during 13 years on the Cocos plate and during 8 years on the Rivera plate. For this purpose, the spatial variations of the Coulomb failure stress resulting from these events have been calculated over extensive areas on the plate interfaces, based on the slip distribution obtained from previous waveform inversion for the corresponding earthquake.

It was found that the rupture nucleation zone of a subsequent event appears to be located in the zone of stress increase due to its previous event, except possibly the case of the 1985 Zihuatanejo event. The Zihuatanejo event was the largest aftershock of the 1985 great Michoacan earthquake and hence, should have been most affected by the mainshock. However, its nucleation zone appears to be located inside the zone of stress decrease or just near the zone of stress increase. This might be due to some uncertainties in the relative location of these two events, their slip patterns, and in the apparent coefficient of friction, etc. We do not have any other reasonable explanations at this moment. For these reasons, the inference on the nucleation zone may not be conclusive. In conclusion, however, the spatio-temporal clustering of the large interplate earthquakes in this subduction zone may possibly be explained primarily by lateral stress interactions due to previous earthquakes located in the adjacent segments on the plate interface.

Acknowledgments

We wish to thank several comments on the present subject given by Shri Krishna Singh and other colleagues at the Instituto de Geofísica, Universidad Nacional Autónoma

de México. We are grateful for the two anonymous reviewers, which improved our original manuscript. This work is partially supported by the CONACYT, Mexico project No. 41209-F. Some work was performed while MAS was under a postdoctoral contract at University of Almería.

Bibliography

- ANDERSON, D. L., 1975. Accelerated plate tectonics. *Science* 187, 1077-1079.
- ANDERSON, O. L. and P. C. GREW, 1977. Stress corrosion theory of crack propagation with application to geophysics. *Rev. Geophys.*, 15, 77-105.
- BABA, T., K. HIRATA and T. HORI, 2005. Afterslip distribution of the 2003 Tokachi-oki earthquake estimated from offshore and onshore geodetic data, 2005 IASPEI meeting, S002-P10.
- DEMETS, C. and D. S. WILSON, 1997. Relative motions of the Pacific, Rivera, North American, and Cocos plates since 0.78 Ma. *J. Geophys. Res.* 102, 2789– 2806.
- DENG, J. and L. R. SYKES, 1997. Evolution of the stress field in southern California and triggering of moderate-size earthquakes: A 200-year perspective. *J. Geophys. Res.* 102, 9859-9886.
- DMOWSKA, R., G. ZENG and J. R. RICE, 1996. Seismicity and deformation at convergence margins due to heterogeneous coupling. *J. Geophys. Res.* 101, 3015-3029.
- FREED, A. M. and J. LIN, 1998. Time-dependent changes in failure stress following thrust earthquakes. *J. Geophys. Res.*, 103, 24,393-24,409.
- HARRIS, R. A., 1998. Introduction to special section: stress triggers, stress shadows, and implications for seismic hazards. *J. Geophys. Res.* 103, 24347-24358.
- HARRIS, R. A. and R. W. SIMPSON, 2002. The 1999 Mw 7.1 Hector Mine, California, earthquake: A test of the stress shadow hypothesis? *Bull. Seism. Soc. Am.*, 92, 1497-1512.
- HEKI, K., S. MIYAZAKI and H. TSUJI, 1997. Silent fault slip following an interplate thrust earthquake at the Japan Trench. *Nature*, 386, 595-598.
- HIROSE, H., K. HIRAHARA, F. KIMATA, N. FUJII, and S. MIYAZAKI, 1999. A slow thrust slip event following the two 1996 Hyuganada earthquakes beneath the Bungo channel. *Geophys. Res. Lett.*, 26, 3217-3240.
- KATO, N., 2004. Interaction of slip on asperities: Numerical simulation of seismic cycles on a two-dimensional planar fault with nonuniform frictional property. *J. Geophys. Res.*, 109, B12306.
- KING, G. C. P., R. S. STEIN and J. LIN, 1994. Static stress changes and the triggering of earthquakes. *Bull. Seism. Soc. Am.* 84, 935-953.
- LEHNER, F. K., V. C. LI and J. R. RICE, 1981. Stress diffusion along rupturing plate boundaries. *J. Geophys. Res.*, 86, 6155-6169.
- MELBOURNE, T., I. CARMICHAEL, C. DEMETS, K. HUDNUT, O. SANCHEZ, J. STOCK, G. SUAREZ, and F. WEBB, 1997. The geodetic signature of the M8.0 Oct. 9, 1995, Jalisco subduction earthquake. *Geophys. Res. Lett.*, 24, 715-718.
- MENDOZA, C., 1993. Coseismic slip of two large Mexican earthquakes from teleseismic body waveforms: Implications for asperity interaction in the Michoacan plate boundary segment. *J. Geophys. Res.*, 98, 8197-8210.
- MENDOZA, C., 1995. Finite fault analysis of the 1979 March 14, Petatlan, Mexico earthquake using teleseismic P waveforms. *Geophys. J. Int.*, 121, 675-683.
- MENDOZA, C. and S. HARTZELL, 1989. Slip distribution of the 19 september 1985 Michoacan, Mexico, earthquake: Near source and teleseismic constraints. *Bull. Seism. Soc. Am.* 79, 655-669.
- MENDOZA, C. and S. HARTZELL, 1997. Fault slip distribution of the 1995 Colima-Jalisco, Mexico, earthquake. *Bull. Seism. Soc. Am.*, 89, 1338-1344.
- MIKUMO, T., T. MIYATAKE and M. A. SANTOYO, 1998. Dynamic rupture of asperities and stress change during a sequence of large interplate earthquakes in the Mexican subduction zone. *Bull. Seism. Soc. Am.* 88, 686-702.
- MIKUMO T., S. K. SINGH and M. A. SANTOYO, 1999. A possible stress interaction between large thrust and normal faulting earthquakes in the Mexican subduction zone. *Bull. Seism. Soc. Am.* 89, 1418-1427.
- MIKUMO, T., Y. YAGI, S. K. SINGH and M. A. SANTOYO, 2002. Coseismic and postseismic stress changes in a

- subducting plate: Possible stress interactions between large interplate thrust and intraplate normal-faulting earthquakes. *J. Geophys. Res.* 107, ESE5-1-ESE5-12.
- MIYAZAKI, S., P. SEGALL, J. FUJITA and T. KATO, 2004. Space time distribution of afterslip following the 2003 Tokachi-oki earthquake: Implications for variations in fault zone friction. *Geophys. Res. Lett.*, 31, L06623, doi:10.29/2003GL019410.
- NISHENKO, S. P. and S. K. SINGH, 1987. Conditional probabilities for the recurrence of large and great interplate earthquakes along the Mexican subduction zone. *Bull. Seism. Soc. Am.* 77, 2095-2114.
- OKADA, Y., 1992. Internal deformation due to shear and tensile faults in a half-space. *Bull. Seism. Soc. Am.* 82, 1018-1040.
- ORTIZ, M., V. KOSTOGLODOV, S. K. SINGH and J. PACHECO, 2000. New constraints on the uplift of October 9, 1995 Jalisco-Colima earthquake (Mw 8) based on the analysis of tsunami records at Manzanillo and Navidad, Mexico. *Geofísica Internacional*, 39, 4, 349-357.
- PARDO, M. and G. SUÁREZ, 1995. Shape of the subducted Rivera and Cocos plates in southern Mexico: seismic and tectonic implications. *J. Geophys. Res.*, 100, 12,357– 12,373.
- POLLITZ, F. F., G. PERTZER and R. BURGMAN, 2000. Mobility of continental mantle: evidence from postseismic geodetic observations following the 1992 Landers earthquake. *J. Geophys. Res.* 105, 8035-8054.
- POLLITZ, F. F. and I. S. SACKS, 2002. Stress triggering of the 1999 Hector Mine earthquake by transient deformation following the 1992 Landers earthquake. *Bull. Seism. Soc. Am.*, 92, 1487-1496.
- REASENBERG, P. A. and R. W. SIMPSON, 1992. Response of regional seismicity to the static stress change produced by the Loma Prieta Earthquake. *Science* 255, 1687-1690.
- RICE, J. R., 1980. The mechanics of earthquake rupture. *In: Physics of the earth's interior*, edited by A. M. Dziewonski and E. Boschi, pp. 555-649, Italian Physical Society/North Holland, Amsterdam.
- RYDELEK, P. and I. S. SACKS, 1990. Asthenosphere viscosity and stress diffusion: a mechanism to explain correlated earthquakes and surface deformations in northeast Japan. *Geophys. J. Int.*, 100, 39-58.
- SANTOYO, M. A., S. K. SINGH, T. MIKUMO and M. ORDAZ, 2005a. Space-time clustering of large thrust earthquakes along the Mexican subduction zone: an evidence of source stress interaction. *Bull. Seism. Soc. Am.* 95, 1856-1864.
- SANTOYO, M. A., T. MIKUMO and LUIS QUINTANAR, 2005b. Faulting process and coseismic stress change during the 30 January, 1973, Colima, Mexico interplate earthquake (Mw=7.6). *Geofísica Internacional*, 45, 163-178.
- SHIRAISHI, A. and S. YOSHIOKA, personal communication.
- SINGH, S. K., L. ASTIZ and J. HAVSKOV, 1981. Seismic gaps and recurrence periods of large earthquake along the Mexican subduction zone: a reexamination. *Bull. Seism. Soc. Am.* 71, 827-843.
- SINGH, S. K. and F. MORTERA, 1991. Source-time functions of large Mexican subduction earthquakes, morphology of the Benioff zone, and the extent of the Guerrero gap. *J. Geophys. Res.*, 96, 21487-21509.
- SINGH, S. K., L. PONCE and S. P. NISHENKO, 1985. The great Jalisco, Mexico, earthquakes of 1932: Subduction of the rivera plate. *Bull. Seism. Soc. Am.* 75, 1301-1313.
- STEIN, R. S., A. BARKA and J. DIETERICH, 1997. Progressive failure of the north Anatolian fault since 1939 by earthquake stress triggering. *Geophys. J. Int.* 128, 594-604.
- STEIN, S., 1999. The role of stress transfer in earthquake occurrence. *Nature*, 402, 605-609.
- TAYLOR, M. A., J. R. DMOWSKA and J. R. RICE, 1998. Upper plate stressing and seismicity in the subduction earthquake cycle. *J. Geophys. Res.*, 103, 24,521-24,542.
- THATCHER, W. and J. B. RUNDLE, 1984. A viscoelastic coupling model for the cyclic deformation due to periodically repeated earthquakes at subduction zones. *J. Geophys. Res.*, 89, 7632-7640.
- VOISIN, C., F. COTTON and S. D. CARLI, 2004. A unified model for dynamic and static stress triggering

of aftershocks, antishocks, remote seismicity, creep events, and multisegment rupture. *J. Geophys. Res.*, 109, B06304, doi:10.1029/2003JB002886.

WARD, S. N., 1992. An application of synthetic seismicity calculations in earthquake statistics: The middle America trench. *J. Geophys. Res.*, 97, 6675-6682.

YAGI, Y., M. KIKUCHI and T. NISHIMURA, 2003. Co-seismic slip, post-seismic slip, and largest aftershock associated with the 1994 Sanriku haruka-oki, Japan, earthquake. *Geophys. Res. Lett.*, 30, doi:10.1029/2003GL018189.

YAGI, Y., T. MIKUMO, J. PACHECO and G. REYES, 2004. Source rupture process of the Tecmán, Colima, Mexico earthquake of 22 January 2003, determined by joint inversion of teleseismic body-wave and near-source data. *Bull. Seism. Soc. Am.*, 94, 1795-1807.

ZIV, A. and A. M. RUBIN, 2000. Static stress transfer and earthquake triggering: no lower threshold in sight?. *J. Geophys. Res.*, 105, 13,631-13,642.

Miguel A. Santoyo^{1,*}, Takeshi Mikumo¹ and Carlos Mendoza²

¹ Instituto de Geofísica, Universidad Nacional Autónoma de México, Mexico City, Mexico.

*Corresponding author: masantoyo@correo.unam.mx

² Centro de Geociencias, Universidad Nacional Autónoma de México, Campus Juriquilla, Querétaro, México.